Solvent frictional forces in the rotational diffusion of proteins in water

Arnab Mukherjee[1] and Biman Bagchi[2,*]

[1]CNRS, UMR 8640, Paris, F-75005 France; Université Pierre et Marie Curie – Paris 6, F-75005, France; Ecole Normale Superieure, Chemistry Department, 24 rue Lhomond, Paris, F-75005 France
[2]Solid State and Structural Chemistry Unit, Indian Institute of Science, Bangalore 560 012, India

Rotational diffusion of a protein is determined largely by its interaction with the surrounding solvent, water. This interaction derives contributions from both the size (short-range interaction) and the charge distribution (long-range interaction) of the protein. Here we show that if the size and shape of the proteins are properly included in the hydrodynamic calculation of Stoke's friction and the correctly estimated charges are used in the calculation of dielectric friction, then the combined friction provides an accurate description of the solvent-induced rotational friction on the proteins. We also discuss the effects of protein–protein interaction in determining the concentration dependence of the rotational diffusion of proteins.

Keywords: Frictional forces, hydration layer, protein rotational diffusion, water.

SEVERAL aspects of the structural and dynamical properties of proteins are determined by the solvent, which is often water. Water determines not only the three-dimensional structure of a protein, but also influences its transport properties, such as rotational and translational diffusion coefficients. Here we investigate and relate the primary aspects of the frictional forces imparted by the solvent on the proteins. Rotational diffusion of proteins has always attracted wide interest because of its accessibility by several different experimental techniques[1,2]. More recently, the rotational diffusion of proteins has attracted renewed attention in the light of the measurement of rotational diffusion in cellular environment and also due to the advent of new experimental techniques such as broadband dielectric spectroscopy and time-dependent dielectric spectroscopy[2]. However, theoretical understanding of rotational diffusion of proteins even in bulk water remains unsatisfactory.

The study of rotational diffusion of proteins in aqueous solution has often been based on Debye–Stokes–Einstein relation (DSE),

$$D_R = \frac{k_B T}{\zeta_R}. \quad (1)$$

*For correspondence. (e-mail: bbagchi@sscu.iisc.ernet.in)

If we approximate the protein molecule as a sphere, then rotational friction ζ_R is given by Stokes relation, $\zeta_R = 8\pi\eta R^3$. Thus, the DSE equation assumes that the protein has a spherical shape, which is often incorrect. There is ambiguity about the determination of some average radius of the protein. If one obtains the radius from the standard mass density of the protein (0.73 g/cc), values of rotational friction are much smaller. The dielectric measurement of South and Grant[3] showed that the experimental value of the rotational friction of myoglobin could only be explained by the above DSE equation if one assumes a thick hydration layer around the protein, thereby increasing the radius of the protein. It is now known that spherical approximation embedded in DSE is grossly in error and the shape of the protein is quite important. However, even with the more recent sophisticated techniques such as tri-axial ellipsoid method[4] and the microscopic bead modelling technique[5,6], which take due recognition of the non-spherical shape of the macromolecule, agreement with the experimental result is not possible without the incorporation of a rigid hydration layer[7].

The assumption of a thick, rigid hydration layer to augment the rotational friction is ambiguous for the following reasons. (i) It has been shown by several studies that there is no such rigid hydration layer around a protein[8]. (ii) Proteins have a heterogeneous surface with a distribution (almost 50 : 50) of hydrophobic and polar or charged amino acid groups. Interaction of these polar and charged groups with the water molecules surrounding the protein can be strong and influential, and certainly different from those with hydrophobic residues. Solvation dynamics on the protein surface umambiguously pointed out this heterogeneity by showing the difference in the lifetime of the hydrogen bond and orientational correlation time near the hydrophobic and hydrophilic residues[9]. Therefore, it is apparent that the concept of a uniform hydration layer is purely ad hoc. (iii) A successful modification to the DSE equation of rotational friction is the tri-axial ellipsoidal method, in which the shape of the protein is assumed to be an ellipsoid. The three different axes of the ellipsoid are the principle axes obtained from diagonalized moment of inertia matrix constructed using the coordinates of the atoms of the protein. However, in order to obtain an agreement with the experimental results, the values of the axes are increased pro-

portionately by increasing the percentage of encapsulation of the protein atoms inside its equivalent ellipsoid[10,11]. A more detailed microscopic approach to the calculation of rotational diffusion coefficient is the bead modelling technique[5]. This technique replaces the atoms by beads of equal sizes and extracts the exact shape of the protein. Then the friction is calculated using hydrodynamic equations. However, exact representation of the shape also is not sufficient to capture the complete effect of the rotational friction on proteins by the solvent. Similar to the assumption of a hydration layer in the case of the DSE and elongation of the axes in the case of the tri-axial method, bead sizes are increased by more than double in this case (3.0 Å instead of 1.2 Å) to account for the effect of the hydration layer[10].

The purpose of the above discussion is to emphasize that while the different approaches of calculation of rotational friction on proteins rely on the additional contribution from the hydration layer of the protein, it is highly approximate. Here we show that this additional contribution results from a completely different source and its origin is not the shape or size, but the charge distribution of proteins, which polarizes the solvent and subsequently faces a reaction field from the solvent, giving rise to what is known as dielectric friction. The dielectric friction (ζ_{DF}) on a protein has been calculated here using a new theoretical formalism using generalized arbitrary charge distribution model (where the charges are obtained from quantum chemical calculation) of the protein. Hydrodynamic friction, on the other hand, is calculated with stick boundary condition, (ζ_{hyd}^{stick}) using a sophisticated theoretical technique known as the tri-axial ellipsoidal method. Calculation of hydrodynamic friction was carried out with only the 'dry volume' of the protein. Here 'dry volume' denotes the volume obtained using the total mass and standard mass density (0.73 g/cc) of the protein and no hydration layer. We show below that the combined effect of hydrodynamic friction thus obtained (without the hydration layer) and the dielectric friction together give rise to the total rotational friction which is in good agreement with the experimentally observed value, i.e. ζ_{total} (= ζ_{DF} + ζ_{hyd}^{stick}) ≈ ζ_{exp}. In addition, we present here an analysis of the size dependence of rotational friction of proteins and discuss the importance of friction due to protein–protein interaction.

Below, we discuss the results obtained on different aspects of rotational friction of proteins. Calculation requires the coordinates of all the amino acid residues of proteins which are obtained from the Protein Data Bank (PDB). Partial charges on the amino acid residues are obtained by quantum chemical calculations using the software Hyperchem.

Hydrodynamic friction

The hydrodynamic rotational friction of the protein depends on its shape and size. Hydrodynamic friction on a rotating rigid body was first estimated by Debye using the well-known DSE relation (eq. (1)). Perrin[12] extended the DSE theory to calculate the hydrodynamic friction for molecules with prolate and oblate-like shapes. Both prolate and oblate have two unequal axes. Harding *et al.*[4] further extended the theory to calculate the hydrodynamic friction using a tri-axial ellipsoid. All the above theories employ stick binary condition to obtain the hydrodynamic friction.

Tri-axial ellipsoidal technique requires the construction of an equivalent ellipsoid of the protein. We have followed the method of Taylor *et al.*[13] to construct an equivalent ellipsoid from the moment matrix. The eigenvalues of this equivalent ellipsoid are proportional to the square of the axes. Thus this method provides two axial ratios. We then obtained the values of the axes using the formula given by Mittelbach[14]:

$$R_\gamma^2 = \frac{1}{5}(A^2 + B^2 + C^3), \tag{2}$$

where R_γ is the radius of gyration and A, B and C are the three unequal axes of a particular protein.

Once the protein is represented as an ellipsoid with three principal axes, the hydrodynamic friction is calculated using Harding's method[4,15]. The hydrodynamic rotational friction of the ellipsoidal axes A, B and C is denoted as ζ_A, ζ_B and ζ_C. The above rotational friction is obtained from the series of equations given below[15],

$$\zeta_0 = 8\pi\eta ABC,$$

$$\zeta_A = \zeta_0 \frac{2(B^2 + C^2)}{3ABC(B^2\alpha_2 + C^2\alpha_3)},$$

$$\zeta_B = \zeta_0 \frac{2(A^2 + C^2)}{3ABC(A^2\alpha_1 + C^2\alpha_3)},$$

$$\zeta_C = \zeta_0 \frac{2(A^2 + B^2)}{3ABC(A^2\alpha_1 + B^2\alpha_2)},$$

$$\alpha_1 = \int_0^\infty \frac{d\lambda}{(A^2 + \lambda)\Delta},$$

$$\alpha_2 = \int_0^\infty \frac{d\lambda}{(B^2 + \lambda)\Delta},$$

$$\alpha_3 = \int_0^\infty \frac{d\lambda}{(C^2 + \lambda)\Delta},$$

$$\Delta = [(A^2 + \lambda)(B^2 + \lambda)(C^2 + \lambda)]^{\frac{1}{2}}, \tag{3}$$

where η is the viscosity of the solvent.

We have calculated the average of tri-axial hydrodynamic friction by taking a simple mean of the friction along three different axes, as given below:

$$\zeta_{\mathrm{TR}}^{\mathrm{av}} = \frac{1}{3}(\zeta_{\mathrm{TR}}^{A} + \zeta_{\mathrm{TR}}^{B} + \zeta_{\mathrm{TR}}^{C}). \quad (4)$$

The values of hydrodynamic friction, along three principal axes (A, B and C) of the ellipsoid and their mean, are tabulated in the Table 1. The A, B and C axes are not the same as the space-fixed X, Y, Z Cartesian reference frame. Note that the values obtained from the tri-axial method are much lower than the experimental values. Here, we can discuss an important aspect of standard hydrodynamic approach – hydration layer. One finds that hydrodynamic values of rotational friction underestimate the rotational friction unless the effect of hydration layer is taken into account. However, the effect of hydration layer is usually incorporated in an ad hoc manner, by increasing the percentage of encapsulation of the atoms inside the ellipsoid[10,11]. In this method, once the two axial ratios are obtained from the equivalent ellipsoid, the actual values of the axes are obtained by increasing the encapsulation of the protein atoms inside the ellipsoid. In the calculation presented here, the axes are obtained by equating with the radius of gyration (eq. (2)). Therefore, we considered no hydration layer in this calculation of hydrodynamic friction. Later, we will show that this effect of hydration layer comes from the dielectric friction.

Dielectric friction

Dielectric friction is known to be an important part of rotational friction for polar or charged molecules in polar solvent, because of polarization of the solvent medium. The solvent molecules, being polarized by the probe, create a reaction field, which opposes rotation of the probe.

Table 1. Stick hydrodynamic friction using tri-axial ellipsoid (in 10^{-23} erg-sec)

Molecule	R_γ (Å)	ζ_{TR}^{A}	ζ_{TR}^{B}	ζ_{TR}^{C}	$\zeta_{\mathrm{TR}}^{\mathrm{av}}$
6pti	11.34	57.8	83.4	85.1	75.4
1ig5	11.36	72.9	78.9	84.9	78.9
1ubq	11.73	71.2	89.9	94.0	85.0
351c	11.51	77.3	84.5	85.3	82.3
1pcs	12.38	78.9	106.5	111.3	98.9
1a1x	13.47	120.8	127.3	143.8	130.6
1gou	13.61	103.3	141.7	148.2	131.1
1aqp	14.45	117.7	171.1	177.0	155.3
1e5y	13.81	108.9	145.7	155.3	136.6
1bwi	13.94	106.9	155.4	158.2	140.1
1b8e	14.70	167.5	172.5	178.2	172.7
4ake	19.59	298.3	422.7	442.8	387.9
3rn3	14.31	112.9	166.5	172.2	150.5
1mbn	15.25	163.7	181.2	210.1	185.0
6lyz	13.97	107.4	156.1	159.1	140.9

Many of the amino acid residues, which constitute the protein, are polar or hydrophilic. Therefore, in the aqueous solution, a protein and other polar molecules experience significant dielectric friction. There exist several theories[16,17], which account for the dielectric contribution to friction. Some of these theories are continuum model calculation of a point charge or point dipole rotating within the spherical cavity. Nee and Zwanzig[16] provided an estimate of the dielectric friction on a point dipole in terms of the dipole moment of the point dipole, dielectric constant of the solvent, Debye relaxation time, and the chosen cavity radius. Later, Alavi and Waldeck[18] extended this theory to incorporate the arbitrary multiple charge distribution of the probe molecule.

Dielectric friction on the proteins has been calculated from the expression of Alavi and Waldeck[18] for arbitrary multiple charge distribution model given below:

$$\zeta_{\mathrm{DF}} = \frac{8}{R_c}\frac{\varepsilon_s - 1}{(2\varepsilon_1 + 1)^2}\tau_{\mathrm{D}} \sum_{j=1}^{N}\sum_{i=1}^{N}\sum_{l=1}^{\infty}\sum_{m=1}^{l}\left(\frac{2l+1}{l+1}\right)\frac{(l-m)!}{(l+m)!}q_i q_j \left(\frac{r_i}{R_c}\right)^l \left(\frac{r_j}{R_c}\right)^l \times m^2 P_l^m(\cos\theta_i) P_l^m(\cos\theta_j)\cos(m\phi_{ji}), \quad (5)$$

where R_c is the cavity radius, (r_i, θ_i, ϕ_i) is the position vector with respect to the centre of mass of the protein and q_i is the partial charge of the ith atom. $P_l^m(\cos(\theta_i))$ is the Legendre polynomial. The maximum value of l used in the Legendre polynomial is 50. ε_s is the static dielectric constant of the solvent. Since the solvent here is water, ε_s is taken to be 78 and the Debye relaxation time τ_{D} is taken as 8.3 picosecond (ps).

Partial charges (q_i) of the atoms constituting the proteins have been calculated using the extended Huckel model of the semi-empirical calculation package of Hyperchem software. The dielectric friction is calculated on each of the atoms in a protein. Rotational friction around X, Y and Z direction is calculated by changing the labels of the atom coordinates. The average dielectric constant $\zeta_{\mathrm{DF}}^{\mathrm{av}}$ is the simple mean of the dielectric friction along X, Y and Z direction. Here X, Y, and Z denote the space fixed Cartesian coordinates of the proteins, as obtained from PDB[19].

Table 2 shows the values of dielectric friction along the X, Y, Z direction and their average. Continuum calculation method of dielectric friction formulated by Alavi and Waldeck[18], is dependent on the cavity radius and has been discussed in detail. They calculated the cavity radius from the observed orientational relaxation time of the organic molecules. The ratios of the longest bond vector of the organic molecules to the cavity radius ranged from 0.75 to 0.85. In Table 2, calculations of dielectric friction are performed using the cavity radius such that the ratio of the longest bond vector to the cavity radius is 0.75.

In Table 3, we compared the average dielectric friction for the two above ratios – 0.75 (denoted as $\zeta_{DF}^{0.75}$) and 0.85 (denoted as $\zeta_{DF}^{0.85}$). $\zeta_{DF}^{0.85}$ is always larger than $\zeta_{DF}^{0.75}$, since shorter cavity radius will put the charges close to the surface of the cavity, thereby increasing the polarization of the solvent and hence the rotational friction of the molecule.

Total friction and rotational diffusion

We now define the total rotational friction as the sum of dielectric friction (ζ_{DF}^{av}) and the hydrodynamic friction without the hydration layer (i.e. tri-axial friction, ζ_{TR}^{av}) as given below[20]:

$$\zeta_{total} = \zeta_{DF}^{av} + \zeta_{TR}^{av}. \quad (6)$$

Diffusion coefficients are obtained from eq. (1). In Table 4, we have shown the values of the average dielectric (ζ_{DF}^{av}), and hydrodynamic (ζ_{TR}^{av}) friction. Total friction (ζ_{total}) defined above, is also shown in Table 4. To compare with the experimental results, we have shown the experimental values of the rotational friction. Note here that while total friction, which is the contribution from both dielectric and hydrodynamic friction, is close to the experimental result, microscopic bead modelling predicts the result which is close to experimental value by itself[6]. The last column in Table 4 shows references from which the experimental results are obtained.

The similarity between the total friction and experimental friction is shown in Figure 1, where we have plotted the experimental values of rotational friction against the total friction for a large number of proteins. For most of the proteins, the results fall on the diagonal line.

From the above results, we can conclude that the sum of dielectric friction and hydrodynamic friction of the dry protein is approximately equal to the experimental results[20].

$$\zeta_{total} \approx \zeta_{exp}. \quad (7)$$

Analysis of size dependence of rotational diffusion of proteins

There are several techniques by which one can measure the rotational diffusion of proteins[21]. These are dielectric dispersion and relaxation, nuclear magnetic and nuclear quadrupole relaxation, ESR line shapes, picosecond pulse techniques, neutron, Raman and depolarized light scattering (DLS), fluorescence depolarization (FD), etc. Since these techniques often measure somewhat different quantities, the results are also different. For example, dielectric relaxation measures the relaxation of the total dipole moment of the protein solution, while fluorescence depolarization studies the relaxation of the second-rank spherical harmonic of a suitably placed probe in protein. The experimental

Table 2. Dielectric friction (in 10^{-23} erg-sec). Cavity radius is chosen such that the ratio of the longest bond vector (R_{max}) of the protein to the chosen cavity radius (R_C) is 0.75

Molecule	R_C (Å)	ζ_{DF}^{X}	ζ_{DF}^{Y}	ζ_{DF}^{Z}	ζ_{DF}^{av}
6pti	29.5	17.8	13.2	18.1	16.4
1ig5	26.1	43.3	36.6	39.1	39.7
1ubq	34.3	18.1	18.3	21.8	19.4
351c	25.5	52.3	41.0	41.9	45.1
1pcs	27.2	90.5	51.3	66.1	69.3
1a1x	33.1	63.0	68.9	49.5	60.5
1gou	32.2	43.8	67.8	103.6	71.7
1aqp	35.3	44.5	71.1	132.1	82.6
1e5y	33.1	98.9	70.6	89.9	86.5
1bwi	35.7	78.3	60.5	108.1	82.3
1b8e	33.5	113.3	112.2	110.5	112.0
4ake	50.3	76.1	170.8	123.4	123.4
3rn3	35.0	118.8	89.0	56.8	88.2
1mbn	28.0	170.7	162.0	160.6	164.5
6lyz	34.0	101.8	77.6	144.0	107.8

Table 3. Cavity size dependence of the dielectric friction (in 10^{-23} erg-sec)

Molecule	$\zeta_{DF}^{0.75}$	$\zeta_{DF}^{0.85}$
6pti	16.4	25.7
1ig5	39.7	61.3
1ubq	19.4	30.3
351c	45.1	69.3
1pcs	69.3	111.0
1a1x	60.5	96.4
1gou	71.7	114.6
1aqp	82.6	132.3
1e5y	86.5	136.4
1bwi	82.3	128.9
1b8e	112.0	174.1
4ake	123.4	211.7
3rn3	88.2	138.1
1mbn	164.5	263.1
6lyz	107.8	172.7

Table 4. Comparison between total friction and experimental results. (Results given in 10^{-23} erg-sec)

Molecule	ζ_{DF}^{av}	ζ_{TR}^{av}	ζ_{total}	ζ_{exp}	Reference
6pti	16.4	75.4	91.8	96.8	29
1ig5	39.7	78.9	118.6	125.0	30
1ubq	19.4	85.0	104.4	118.9	31
351c	45.1	82.3	127.4	130.1	32
1pcs	69.3	98.9	168.2	149.5	33
1a1x	60.5	130.6	191.1	241.9	34
1gou	71.7	131.1	202.8	191.3	35
1aqp	82.6	155.3	237.9	186.1	36
1e5y	86.5	136.6	223.1	190.4	37
1bwi	82.3	140.1	222.4	203.6	38
1b8e	112.0	172.7	284.7	270.6	39
4ake	123.4	387.9	511.3	478.2	40
3rn3	88.2	150.5	238.7	235.0	41
1mnb	164.5	185.0	349.5	246.3	3
6lyz	107.8	140.9	248.7	172.8	42

results quoted here are from ^{15}N relaxation study, FD and DLS.

In Figure 2, we have plotted the experimental results of rotational diffusion (D_R^{EXP}) against the radius of gyration of proteins – the latter is calculated from the X-ray or NMR structure of the protein. The values of D_R^{EXP} can be fitted to a power-law expression as follows:

$$D_R = PR_\gamma^{-\alpha}, \tag{8}$$

where P is the prefactor. The above equation becomes the same as eq. (1) if $P = \frac{k_B T}{8\pi\eta}$ and $\alpha = 3.0$. At 293 K, and in water, the value of P from the DSE is equal to 16.1×10^{-14}.

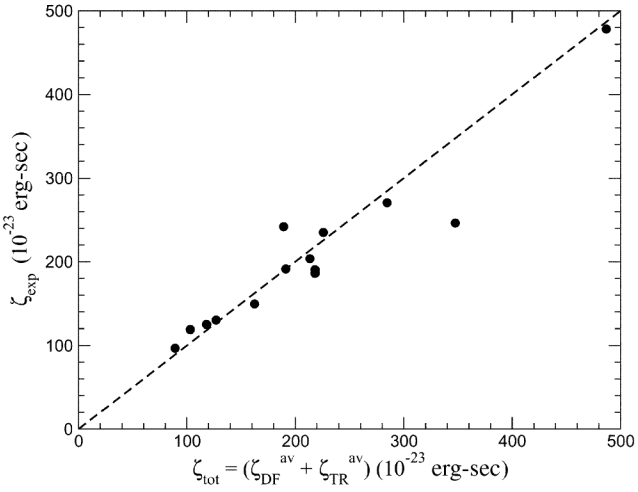

Figure 1. Combined friction from hydrodynamic and dielectric plotted against experimental results. Solid line shows diagonal to guide the eye.

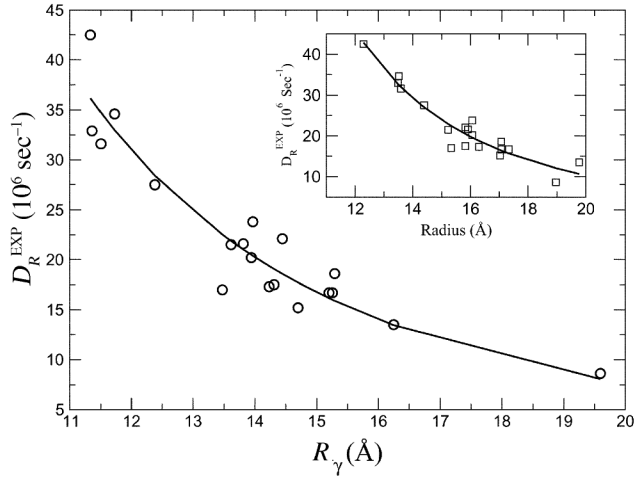

Figure 2. Experimental rotational diffusion (D_R^{EXP}) coefficients are plotted against the calculated R_γ for some proteins. Circles show experimental values and solid line is the power law fit with an exponent 2.75. (Inset) Squares show plot of D_R^{EXP} against radius of the protein obtained from total mass. Solid line is a power-law fit, with an exponent 2.92.

The exponent α obtained from the fitting (shown in Figure 3) is 2.75 and $P = 5.02 \times 10^{-14}$.

Our work was further motivated by a recent report that R_γ can provide a useful measure for structure determination[22]. The study showed that R_γ values calculated from NMR and X-ray structures of the protein are almost similar. In a globular protein, R_γ can be predicted with reasonable accuracy on the basis of the number of amino acid residues using the following relationship[23]:

$$R_\gamma^{predict} = 2.2N\zeta_R^{0.38}, \tag{9}$$

where N_R is the number of residues in a protein. It has been shown by Huang and Powers[22] that $R_\gamma^{predict} \approx R_\gamma$. Now using eqs (8) and (9), we can obtain the relation between the rotational discussion coefficients of a protein with the number of residues as given below:

$$D_R = P\ 2.2^{-\alpha} N_R^{-\beta}, \tag{10}$$

where $\beta \approx 1$.

Thus,

$$D_R \propto \frac{1}{N_R}. \tag{11}$$

This result was not expected for a globular protein, especially in view of the failure of eq. (1). Therefore, we have also fitted the experimental results to the radius and found a similar correlation (shown in the inset, Figure 2) with radius R, where R is calculated from the exact mass along with the mass density of 0.73 g/cc. The fit is quite good with exponent 2.92, instead of 3. The prefactor is substantially different from the one given by the DSE relation (eq. (1)).

The above fit reminds one of the argument put forward by Zwanzig and Harrison[24], who observed that one should use an effective hydrodynamic radius when employing the simple Stokes expression to calculate the transport properties. We show below that accurate methods developed recently, can indeed reproduce the weaker than R^{-3} dependence of rotational diffusion on R_γ.

The size, shape and charge distribution of proteins give rise to two different contributions to the rotational friction. The former is called hydrodynamic friction, while the latter is known as dielectric friction. We now discuss the methods involved in the calculation of the above two different contributions to rotational friction.

In Figure 3, we have plotted the average dielectric and hydrodynamic friction against radius for various proteins. Frictional values obtained from experiments are also plotted in the same graph for comparison. Note that while hydrodynamic friction has the predictable dependence on radius of the protein, dielectric friction behaves differently.

This is expected since dielectric friction arises from the charge distribution and electric field, not directly related to the size or the shape of the protein. As shown earlier,

the combined effect of dielectric and hydrodynamic friction equals to the rotational friction calculated using experiments. Figure 4 plots the rotational diffusion coefficient obtained from both experiment and theory, against radius of the protein. Note the satisfactory agreement, particularly in view of the fact that we have used no adjustable parameter.

Effects of protein–protein interactions on rotational diffusion

Protein molecules are typically much larger in size than the solvent water molecules. They are, however, smaller than typical colloids where hydrodynamic interaction (HI) is important in determining viscosity. However, the size of the proteins is sufficiently large to make the effects of HIs important. In addition, protein side chains are charged and polar. This means that two protein molecules can interact via the Coulombic force, which is long-ranged. Therefore, we can immediately identify two sources of interaction among proteins which can affect rotational diffusion of proteins. We can approximately address the effects of HI by combining Einstein's relation for viscosity with friction. Einstein's relation for viscosity augmentation due to HI is given by[25]:

$$\eta(\phi) = \eta_0 + \frac{5}{2}\phi + O(\phi^2), \tag{12}$$

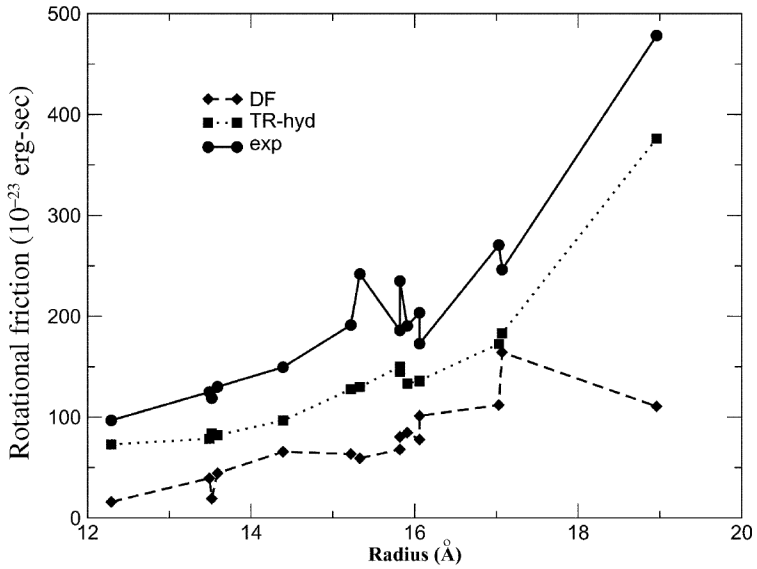

Figure 3. Rotational friction coefficients obtained from the experiment, hydrodynamic and dielectric friction plotted against radius for some proteins.

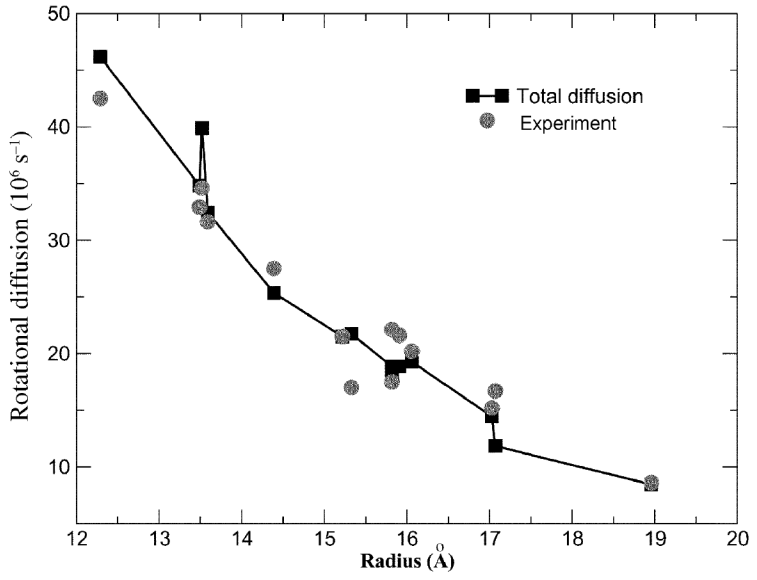

Figure 4. Experimental rotational friction coefficients and total friction plotted against radius.

where ϕ is the volume fraction of proteins and η_0 is the viscosity of neat water. The above expression assumes no specific interaction between the solute and the solvent[25]. Thus, the above equation predicts an increase in rotational friction and decrease in rotational diffusion with concentration.

HI is a dynamic effect. The effects of static interaction due to charged and the polar groups on the protein surface are more difficult to account for. q_{Ai} and q_{Bj} denote the charges of the ith and jth atoms of protein A and B respectively. $\mathbf{r}_{Ai}$ and $\mathbf{r}_{Bi}$ denote the position of the ith atom of protein A and B respectively. The Coulombic interaction between the two proteins can be written as:

$$V_{AB}(R) = \sum_{i,j} \frac{q_{Ai} q_{Bj}}{\varepsilon \mid \mathbf{r}_{Ai} - \mathbf{r}_{Bj} \mid}, \tag{13}$$

where we have assumed the protein molecule to be spherical, for this part of the discussion. Here ε is the static dielectric constant of water.

At low concentration, when protein molecules are far away from each other, we can replace the discrete charges by a dipole moment placed at the centre of the sphere. Dipole moments of protein molecules has been computed in several studies[8]. It can also be calculated by semi-empirical methods. The value of the dipole moment is quite large for proteins, reflecting the presence of many polar and charged groups. Thus, if we assume a dipole–dipole interaction, then we can define the usual dimensionless interaction parameter $3Y = \mu_P^2 \rho_p / 3\varepsilon k_B T$, where ρ_P is the number density of protein molecules in solution[26]. Since μ_P is large, this value can be significant even at low protein concentration.

Since the protein rotation is much slower and expected to be decoupled from solvent dynamics, we can calculate the dielectric friction due to inter-protein interactions using a molecular theory, like a mode coupling theory of rotational dielectric friction[27]. Note that a continuum model calculation will fail to incorporate this effect as it will get masked by the contribution of water to dielectric friction. However, a molecular theory can include only the inter-protein correlations. Detailed calculation of this friction using mode coupling theory is under progress.

However, one can draw a few conclusions from theoretical considerations straightaway. The rotational correlation function of the protein may exhibit a slow decay due to interprotein interactions. The effect of this slow decay on total friction is not negligible.

Conclusion

Let us first summarize the main results of this work. We have calculated the rotational diffusion of a large number of proteins using Einstein's relation which correlates the rotational friction to the rotational diffusion constant – the latter is related to the experimentally observed rotational correlation time by a well-known expression. Next, we have assumed that the total rotational friction can be decomposed into a sum of two terms – the hydrodynamic friction and the dielectric friction. We have calculated the hydrodynamic rotational friction on proteins using the tri-axial ellipsoid method, formulated by Harding *et al.*[4], and the dielectric friction using the generalized charge distribution model derived by Alavi and Waldeck[18]. The hydrodynamic friction is calculated without the inclusion of any hydration layer. We have found that the combined effect of dielectric and hydrodynamic friction gives an estimate which is surprisingly close to the experimental result. This approach seems to provide a microscopic basis for the standard hydrodynamic approach, where a hydration layer is added to the protein in an ad hoc manner, to calculate rotational friction.

In addition, we have shown using experimental results and two different theoretical techniques that the total rotational diffusion coefficients scale with radius of gyration. Exponent of the power law fit varies from 2.75 to 2.9. Data can also be fitted to a variation in the effective radius with similar power law. However, the prefactor obtained by fitting is quite different from that predicted by the DSE. Using the relation of radius of gyration and the number of residues for a globular protein, we have shown that rotational diffusion coefficient is inversely proportional to the number of residues for a globular protein.

The weaker dependence of rotational friction on the radius (of gyration) may be due to several factors. First, the larger proteins are usually more oblate than prolate. Second, the side chains of the protein molecules are mobile on the timescale of rotation. This is an interesting problem for study. Use of the stick boundary condition may itself be flawed. It seems to compensate for the neglect of the dielectric friction. It is notable that the success of the microscopic bead modelling technique depends critically on the enhanced size of the protein. This is another interesting issue that remains to be explored.

The calculations adopted here are still not without limitations. The continuum calculation of dielectric friction is dependent on the assumed a cavity radius. Unfortunately, there is yet no microscopic basis to assume a certain value of the cavity radius for the calculation of dielectric friction. Moreover, the effect of increasing dielectric constant of the solvent from the vicinity of the protein to the bulk is not taken into account by Alavi and Waldeck[18]. Thus, we have attempted to incorporate a multi-shell model to incorporate multiple shells with varying dielectric constants.

Similarly, the tri-axial method still suffers from the lack of microscopic basis to determine the exact values of the axes respectively.

A potentially powerful approach to the problem is the mode coupling theory[27], which uses the time correlation formalism to obtain the memory kernel of the rotational

friction. The total torque is separated into two parts – a short-range part (which is called the bare friction Γ_{bare}) and a long-range dipolar part. The advantage of mode coupling theory is that it does not depend on any parameter. It uses a time-dependent effective potential field in terms of density distribution and direct correlation function. For a spherical ion, this potential can be given by[27],

$$V_{\text{eff}}(\mathbf{r}, \Omega, t) = -k_B T \int \mathrm{d}r' d\Omega' c(\mathbf{r}-\mathbf{r}', \Omega, \Omega') \nabla_{\Omega\rho}(r', \Omega', t). \tag{14}$$

The torque density is then expressed as:

$$N_c(\mathbf{r}, \Omega, t) = n(\mathbf{r}, \Omega, t)[-\nabla_\Omega V_{\text{eff}}(\mathbf{r}, \Omega, t)], \tag{15}$$

where $n(\mathbf{r}, \Omega, t)$ is the number density of the tagged particle. The rotational friction comes from the torque–torque correlation function. The final expressions of the single particle (Γ_s) and collective friction (Γ_c) are given by[28]:

$$\Gamma_s(z) = \Gamma_{\text{bare}} + A \int_0^\infty \mathrm{e}^{-zt} \int_0^\infty \mathrm{d}k\, k^2 \sum_{l_1 l_2 m} c^2_{l_1 l_2 m}(k) F_{l_2 m}(k, t), \tag{16}$$

$$\Gamma_c(z) = \Gamma_{\text{bare}} + A \int_0^\infty \mathrm{e}^{-zt} \int_0^\infty dk\, k^2 \sum_{l_1 l_2 m} F^s_{l_1 m}(k, t) c^2_{l_1 l_2 m}(k) F_{l_2 m}(k, t), \tag{17}$$

where $A = \rho/2(2\pi)^4$. $c_{l_1 l_2 m}$ is the $l_1 l_2 m$th coefficient of the two-particle direct correlation function between any two dipolar molecules. $F^s_{l_1 l_2 m}$ and $F_{l_2 m}(k, t)$ are the single particle and collective orientational correlation functions respectively.

Equations (13) and (14) are the standard mode coupling theory expressions for rotational friction. They have to be solved self-consistently. In the overdamped limit, the self-dynamic structure factor is expressed as:

$$F^s_{lm}(k, z) = \left[z + \frac{k_B T l(l+1)}{l\Gamma_s(z)} \right]^{-1}, \tag{18}$$

and the collective dynamic structure factor is given by,

$$F^c_{lm} = F_{lm}(k) \left[z + \frac{k_B T f_{llm}(k) l(l+1)}{I\Gamma_c(z)} + \frac{k_B T k^2 f_{llm}(k)}{M\Gamma_T(z)} \right]^{-1}, \tag{19}$$

where $f_{llm}(k) = 1-(-1)^m(\rho/4\pi)c_{llm}(k)$. I and M are moment of inertia and mass of the dipolar molecule respectively. $\Gamma_T(z)$ is the frequency-dependent translational friction.

The difficulty of applying such a formalism to calculate friction on protein is manifold. First, one needs to obtain the protein–water direct correlation function. Second, the k-space description itself may not be appropriate, or needs modification.

1. Krushelnitsky, A., Intermolecular electrostatic interactions and Brownian tumbling in protein solutions. *Phys. Chem. Chem. Phys.*, 2006, **8**, 2117–2128.
2. Feldman, Y., Ermolina, I. and Hayashi, Y., Time domain dielectric spectroscopy study of biological systems. *IEEE Trans. Dielectr. Electr. Insul.*, 2003, **10**, 728– 753.
3. South, G. P. and Grant, E. H., Dielectric dispersion and dipole-moment of myoglobin in water. *Proc. R. Soc. London, Ser. A*, 1972, **328**, 371.
4. Harding, S. E., Dampier, M. and Rowe, A. J., Modelling biological macromolecules in solution: the general triaxial ellipsoid can now be employed. *IRCS Med. Sci.*, 1979, **7**, 33.
5. de la Torre, J. G., Hydration from hydrodynamics. General considerations and applications of bead modelling to globular proteins. *Biophys. Chem.*, 2001, **93**, 159–170.
6. Garcia de la Torre, J., Huertas, M. and Carrasco, B., Calculation of hydrodynamic properties of globular proteins from their atomic-level structure. *Biophys. J.*, 2000, **78**, 719–730.
7. Carrasco, B. and de la Torre, J. G., Hydrodynamic properties of rigid particles: Comparison of different modeling and computational procedures. *Biophys. J.*, 1999, **76**, 3044–3057.
8. Nandi, N. and Bagchi, B., Dielectric relaxation of biological water. *J. Phys. Chem. B*, 1997, **101**, 10954–10961.
9. Russo, D., Hura, G. and Head-Gordon, T., Hydration dynamics near a model protein surface. *Biophys. J.*, 2004, **86**, 1852–1862.
10. Harding, S. E., The hydration problem in solution biophysics: an introduction. *Biophys. Chem.*, 2001, **93**, 87–91.
11. Muller, J. J., Prediction of the rotational diffusion behavior of biopolymers on the basis of their solution or crystal structure. *Biopolymers*, 1991, **31**, 149–160.
12. Perrin, F. J., *Phys. Radiat. Ser.*, 1934, **VII 5**, 497.
13. Taylor, W. R., Thornton, J. M. and Turnell, W. G., An ellipsoidal approximation of protein shape. *J. Mol. Graphics*, 1983, **1**, 30–38.
14. Mittelbach, P., Zur Roentgenkleinwinkelstreuung verdunter kolloider Systeme. VIII. Diskussion des Streuverhaltens regelmaessiger Koerper und Methoden zur Bestimmung von Groesse und Form kolloider Teilchen. *Acta Phys. Austriaca*, 1964, **19**, 53–102.
15. Harding, S. E., A computer program for evaluating the hydrodynamic parameters of a macromolecule in solution for any given value of its axial dimensions. *Comp. Biol. Med.*, 1982, **12**, 75–80.
16. Nee, T. W. and Zwanzig, R., Theory of dielectric relaxation in polar liquids. *J. Chem. Phys.*, 1970, **52**, 6353.
17. Hubbard, J. B., Friction on a rotating dipole. *J. Chem. Phys.*, 1978, **69**, 1007–1009.
18. Alavi, D. S. and Waldeck, D. H., Rotational dielectric friction on a generalized charge distribution. *J. Chem. Phys.* 1991, **94**, 6196–6202.
19. Bernstein, F. C. *et al.*, Protein Data Bank – Computer-based archival file for macromolecular structures. *J. Mol. Biol.*, 1977, **112**, 535–542.
20. Mukherjee, A. and Bagchi, B., Rotational friction on globular proteins combining dielectric and hydrodynamic effects. *Chem. Phys. Lett.*, 2005, **404**, 409–413.
21. Berne, B. J. and Pecora, R., *Dynamic Light Scattering*, John Wiley, 1976.
22. Huang, X. M. and Powers, R., Validity of using the radius of gyration as a restraint in NMR protein structure determination. *J. Am. Chem. Soc.*, 2001, **123**, 3834–3835.
23. Skolnick, J., Kolinski, A. and Ortiz, A. R. MONSSTER: A method for folding globular proteins with a small number of distance restraints. *J. Mol. Biol.*, 1997, **265**, 217–241.
24. Zwanzig, R. and Harrison, A. K., Modifications of the Stokes–Einstein formula. *J. Chem. Phys.*, 1985, **83**, 5861–5862.
25. Verberg, R., de Schepper, I. M. and Cohen, E. G. D., Viscosity of colloidal suspensions. *Phys. Rev. E*, 1997, **55**, 3143–3158.

26. Hansen, J. P. and McDonald, I. R., *Theory of Simple Liquids*, Academic Press, New York, 1986.
27. Bagchi, B. and Chandra, A., Collective orientational relaxation in dense dipolar liquids. *Adv. Chem. Phys.*, 1991, **80**, 1–126.
28. Bagchi, B., Self-consistent molecular theory of orientational relaxation and dielectric friction in a dense dipolar liquid. *J. Mol. Liq.*, 1998, **77**, 177–189.
29. Beeser, S. A., Goldenberg, D. P. and Oas, T. G., Enhanced protein flexibility caused by a destabilizing amino acid replacement in BPTI. *J. Mol. Biol.*, 1997, **269**, 154–164.
30. Kordel, J., Skelton, N., Akke, M., Palmer, 3rd, A. and Chazin, W., Backbone dynamics of calcium-loaded calbindin D9k studied by two-dimensional proton-detected 15N NMR spectroscopy. *Biochemistry*, 1992, **31**, 4856–4866.
31. Tjandra, N., Feller, S. E., Pastor, R. W. and Bax, A., Rotational diffusion anisotropy of human ubiquitin from N-15 NMR relaxation. *J. Am. Chem. Soc.*, 1995, **117**, 12562–12566.
32. Russell, B., Zhong, L., Bigotti, M., Cutruzzola, F. and Bren, K., Backbone dynamics and hydrogen exchange of *Pseudomonas aeruginosa* ferricytochrome c(551). *J. Biol. Inorg. Chem.*, 2003, **8**, 156–166.
33. Bertini, I. *et al.*, Backbone dynamics of plastocyanin in both oxidation states – Solution structure of the reduced form and comparison with the oxidized state. *J. Biol. Chem.*, 2001, **276**, 47217–47226.
34. Guignard, L., Padilla, A., Mispelter, J., Yang, Y. S., Stern, M. H., Lhoste, J. M. and Roumestand, C., Backbone dynamics and solution structure refinement of the N-15-labeled human oncogenic protein p13(MTCP1): Comparison with X-ray data. *J. Biomol. NMR*, 2000, **17**, 215–230.
35. Pang, Y., Buck, M. and Zuiderweg, E. R. P., Backbone dynamics of the ribonuclease binase active site area using multinuclear (N-15 and (CO)-C-13) NMR relaxation and computational molecular dynamics. *Biochemistry*, 2002, **41**, 2655–2666.
36. Cole, R. and Loria, J. P., Evidence for flexibility in the function of ribonuclease A. *Biochemistry*, 2002, **41**, 6072–6081.
37. Kalverda, A. P., Ubbink, M., Gilardi, G., Wijmenga, S. S., Crawford, A., Jeuken, L. J. C. and Canters, G. W., Backbone dynamics of azurin in solution: Slow conformational change associated with deprotonation of histidine 35. *Biochemistry*, 1999, **38**, 12690–12697.
38. Buck, M. *et al.*, Structural determinants of protein dynamics – analysis of N-15 NMR relaxation measurements for main-chain and side chain nuclei of hen egg-white lysozyme. *Biochemistry*, 1995, **34**, 4041–4055.
39. Uhrinova, S., Smith, M. H., Jameson, G. B., Uhrin, D., Sawyer, L. and Barlow, P. N., Structural changes accompanying pH-induced dissociation of the beta-lactoglobulin dimer. *Biochemistry*, 2000, **39**, 3565–3574.
40. Shapiro, Y. E., Sinev, M. A., Sineva, E. V., Tugarinov, V. and Meirovitch, E., Backbone dynamics of *Escherichia coli* adenylate kinase at the extreme stages of the catalytic cycle studied by N-15 NMR relaxation. *Biochemistry*, 2000, **39**, 6634–6644.
41. Keefe, S. E. and Grant, E. H., Dipole-moment and relaxation-time of ribonuclease. *Phys. Med. Biol.*, 1974, **19**, 701–707.
42. Dubin, S. B., Clark, N. A. and Benedek, G. B., Measurement of rotational diffusion coefficient of lysozyme by depolarized light scattering-configuration of lysozyme in solution. *J. Chem. Phys.*, 1971, **54**, 5158.

ACKNOWLEDGEMENT. This work is supported by DST, DBT and CSIR, New Delhi and partly supported by CEFIPRA, EGIDE, France.

Received 7 July 2006; accepted 1 September 2006